Available online at www.sciencedirect.com
ScienceDirect
Combustion and Flame 154 (2008) 67–81
Combustion and Flame
www.elsevier.com/locate/combustflame

An efficient error-propagation-based reduction method for large chemical kinetic mechanisms

P. Pepiot-Desjardins *, H. Pitsch

Department of Mechanical Engineering, Stanford University, Stanford, CA, USA

Received 2 July 2007; received in revised form 1 October 2007; accepted 18 October 2007

Available online 3 January 2008

Abstract

Production rates obtained from a detailed chemical mechanism are analyzed in order to quantify the coupling between the various species and reactions involved. These interactions can be represented by a directed relation graph. A geometric error propagation strategy applied to this graph accurately identifies the dependencies of specified targets and creates a set of increasingly simplified kinetic schemes containing only the chemical paths deemed the most important for the targets. An integrity check is performed concurrently with the reduction process to avoid truncated chemical paths and mass accumulation in intermediate species. The quality of a given skeletal model is assessed through the magnitude of the errors introduced in the target predictions. The applied error evaluation is variable-dependent and unambiguous for unsteady problems. The technique yields overall monotonically increasing errors, and the smallest skeletal mechanism that satisfies a user-defined error tolerance over a selected domain of applicability is readily obtained. An additional module based on life-time analysis identifies a set of species that can be modeled accurately by quasi-steady state relations. An application of the reduction procedure is presented for autoignition using a large iso-octane mechanism. The whole process is automatic, is fast, has moderate CPU and memory requirements, and compares favorably to other existing techniques.

Keywords: DRGEP; Chemical kinetics reduction; Skeletal chemistry; Autoignition; Iso-octane

1. Introduction

Cost and efficiency drive the design of combustion devices to rely more and more on numerical simulations. As the methods for computational fluid dynamics (CFD) progress, complex problems such as the simulation of chemically reactive flows in engines become tractable. Of interest, for instance, is the capability to accurately predict pollutant emissions from engines, for which the understanding and the accurate modeling of chemistry are tremendously important. Combustion of fossil fuels involves complex highly nonlinear processes involving hundreds of different chemical compounds. Detailed chemical models for real hydrocarbon fuels are therefore very difficult to derive and the fuel representation needs to be simplified drastically to be included in numerical simulations of combustion devices.

A first stage of simplification consists of approximating the fuel by a well-defined mixture of a few components that will match some physical or chemical properties of the real fuel such as hydrogen-

* Corresponding author.
E-mail address: pepiot@stanford.edu (P. Pepiot-Desjardins).

0010-2180/$ – see front matter
doi:10.1016/j.combustflame.2007.10.020

to-carbon ratio, density, or boiling characteristics. Using surrogate fuels in lieu of real fuels presents numerous advantages, among which are the reproducibility of experiments and the possibility of formulating chemical models suitable for CFD. Recent progress in formulating appropriate surrogate compositions has been made for gasoline [1], diesel [2], and jet fuels [3,4]. Examples of surrogates include *n*-butylbenzene, *n*-butylcyclohexane, and *n*-decane for jet fuels, or mixtures of *n*-heptane, iso-octane, and toluene for gasoline.

The chemistry of each component in a given surrogate can be modeled by detailed chemical kinetic reaction mechanisms involving hundreds of species and thousands of reactions. Although the available computational power is growing fast, simplification of these detailed mechanisms is essential for their use in CFD codes. Powerful short mechanisms [5,6] have been derived manually, often by combining chemical intuition with tools such as sensitivity and flux analysis. However, the growing size of the mechanisms does not allow for such approaches anymore. Thus, developing reliable automatic reduction methods that require minimum user input is a necessity, and major advancements have been made on this topic recently.

Overviews of existing reduction methods can be found in a number of references [7–9]. Basically, reduction can be performed at two different levels. The first stage aims at removing explicitly species [7,10–14] and reactions [15–17] that have a negligible contribution to the phenomena of interest. Then the resulting skeletal mechanism is suitable for other techniques introducing model assumptions to further accelerate the computation. These techniques are usually based on time-scale analysis, such as quasi-steady-state assumptions (QSSA) [18], Intrinsic low-dimensional manifolds (ILDM) [19], or computational singular perturbation (CSP) [20]. The following work concentrates mostly on designing a reliable tool for the systematic reduction of mechanisms to a skeletal level.

1.1. Prereduction considerations

Several steps are involved in the development of a skeletal mechanism. The first is the development of a detailed chemical kinetic reaction mechanism, which can in principle be considered as independent of the reduction procedure. However, the validation of the detailed mechanism has a very strong connection to the subsequent reduction procedure. First of all, the validation sets a range of validity and applicability for the detailed mechanism. Any reduced mechanism will also be applicable in the same range of parameters and configurations. Second, the validation procedure of the detailed mechanism will reveal a certain error when compared with experiments. This error might influence the choice of the accuracy requirements in the reduction procedure. For example, if the detailed mechanism reproduces the experimental data with very good accuracy, the reduced scheme should retain this desirable property, and the error tolerances in those regions could be more stringent than in regions in which experimental data are not well reproduced by the detailed model. The goal of the reduction is to develop a reduced scheme that represents, up to a specified error, certain features of the detailed mechanism in its range of applicability.

1.2. DRG and CSP methods

The next step in the reduction procedure is therefore the choice of a set of targets. The targets are some desirable chemical features that the reduced mechanism is expected to reproduce over a predefined range of physical conditions. The targets can be as diverse as ignition properties, burning velocities, and levels of soot precursors. Thus, a reference database can be obtained by computing the solutions for a number of sample cases pertaining to the applicability domain using the detailed mechanism. This database is analyzed to quantify couplings between species. Two existing methods are emphasized next, which are similar in structure but differ in the type of analysis that is done using the detailed or reference solution: the directed relation graph (DRG) method [10,21], which is based on production rate analysis, and a method that relies on time scale analysis using the CSP theory [7,22–24]. The latter uses a decomposition of the solution into fast and slow subspaces. The solution vector is assumed to evolve along the slow subspace or manifold according to the slow time scales and to be constrained on this surface by the faster processes. In both DRG and CSP methods, the results of the analysis can be represented by a directed relation graph whose nodes are the species. In the DRG method, the strength of the directed edge linking a species A to another species B is proportional to the contribution of B in the production rate of A. In the CSP method on the other hand, the strength of this edge depends on the contribution to the slow and the fast subspaces of the elementary reactions involving both A and B, so that the rapid evolution toward the slow manifold and the slow evolution on this manifold are represented correctly.

For a given value of a user-defined parameter representing the desired degree of reduction, the graph is simplified to include only those edges whose strength is larger than this parameter, and all species reachable from the targets through this graph are included in the resulting skeletal mechanism. Variations of this selection process have been designed and tested for

the CSP method by Valorani et al. [24]. The procedure is applied for each sample point and the resulting sets are concatenated into one single global set. Both methods require only a single evaluation of the solution using the detailed mechanism, and once the initial graph has been constructed, the selection process is fast for both approaches.

However, in both the selection procedures of DRG and those of CSP, it is assumed that every species selected to be kept in the mechanism is equally important and that the set of strongly coupled species to which it belongs has to be kept entirely, which may not be necessary. To apply a finer selection, the directed relation graph with error propagation (DRGEP) method is presented here, which postulates that the influence of an error introduced by the change of the concentration of a species, or by discarding the species entirely, is damped as it propagates along the graph to reach the targets. As pointed out by Lu and Law [25], the geometric damping proposed in [26] using the DRG coupling coefficients failed to identify long chemical paths involving fast processes and quasi-steady state intermediate species. A new definition of the coupling coefficient is described here that addresses this issue. Also, the selection procedure is designed to avoid any truncated chemical path in the skeletal mechanism that would introduce mass accumulation in intermediate species, thus creating large discrepancies in the concentration of products. Similar procedures are employed to reduce both the number of species and the number of reactions. An additional module allows the selection of suitable quasi-steady state species, and an unambiguous error measure is defined for unsteady simulations.

2. DRGEP methodology

The goal of the reduction procedure is to identify, for any number of species in the skeletal mechanism, N_{skel}, a group of species of size $N_{\text{rm}} = N_{\text{det}} - N_{\text{skel}}$ that can be removed with minimal impact on the targets. This is done here by defining appropriate importance coefficients for each species based on the production and consumption rates, which are evaluated using results obtained from the detailed mechanism. The species with the N_{rm} lowest importance coefficients are then removed from the mechanism and a skeletal mechanism of size N_{skel} is created by removing from the detailed mechanism any reaction in which a removed species appears as reactant or as product. In the remaining part of this section, the definition of the importance coefficients will be described.

2.1. Direct interaction coefficients

Direct interaction coefficients are defined as the measure of the coupling between two species that are directly related through an elementary reaction, that is, two species that appear concurrently in the same reaction. In the DRG method, the coupling coefficient between two directly related species A and B is estimated as:

$$r_{AB}^{\text{DRG}} \equiv \frac{\sum_{i=1,n_{\text{R}}} |\nu_{i,A}\omega_i \delta_B^i|}{\sum_{i=1,n_{\text{R}}} |\nu_{i,A}\omega_i|}, \tag{1}$$

where

$$\begin{aligned}\omega_i &= \omega_{\text{f},i} - \omega_{\text{b},i} \\ &= k_{\text{f},i} \prod_{j=1}^{n_{\text{E},i}} [S_j]^{\nu'_{i,j}} - k_{\text{b},i} \prod_{j=1}^{n_{\text{P},i}} [S_j]^{\nu''_{i,j}}.\end{aligned} \tag{2}$$

Here, n_{R} is the total number of reversible reactions in the mechanism, and $\omega_{\text{f},i}$, $\omega_{\text{b},i}$, and ω_i are the forward, backward, and net reaction rates of the ith reaction, respectively. $\nu'_{i,j}$ and $\nu''_{i,j}$ are the stoichiometric coefficients of species j in reaction i on the reactants and products sides, respectively, and $\nu_{i,j} = \nu''_{i,j} - \nu'_{i,j}$ is the net stoichiometric coefficient of species j in reaction i. $n_{\text{E},i}$ and $n_{\text{P},i}$ are the numbers of educts and products in reaction i, respectively. $k_{\text{f},i}$ and $k_{\text{b},i}$ are the rate coefficients of the forward and backward parts of the ith reaction. $k_{\text{b},i}$ is either computed from the equilibrium constant, which is given by thermodynamic properties, or expressed explicitly in Arrhenius form in the mechanism. δ_B^i is defined as

$$\delta_B^i = \begin{cases} 1, & \text{if the } i\text{th reaction involves species } B, \\ 0, & \text{otherwise.} \end{cases} \tag{3}$$

If A and B are directly related, then both r_{AB} and r_{BA} exist, are nonzero, and generally are not equal. Whenever a graph is displayed in the following, r_{AB}, representing the influence of species B on species A, will be represented schematically as a directed arrow from A to B. The definition given in Eq. (1) is an estimate of the error made in the prediction of species A if species B is neglected. Production and consumption reactions are considered equally. However, removing a species that contributes exclusively to the consumption of the target A will not have the same effect as removing a species that contributes the same amount to the production and to the consumption of A. For the same value of the coefficient r_{AB}^{DRG}, the first species will introduce a larger error in the net production rate of A than the latter, which might introduce virtually no error. The reason is that in the latter case, a part of the error from removing the production term is compensated for by also removing the associated consumption term. This example stresses

the fact that a more accurate quantity to consider is the net contribution of species B to species A, rather than production and consumption individually.

Other alternative definitions of the direct interaction coefficient were discussed by Lu and Law [25]. These definitions include normalizing the coefficient by the net production rate of species A, which becomes singular when A approaches steady state, or considering backward and forward reactions as distinct, which fails when the rate-controlling reaction is dominated by a fast pseudo-equilibrium (PE) reaction.

Here, a new definition of the direct interaction coefficient is introduced, which is motivated by the shortcomings of earlier formulations, namely,

$$r_{AB} \equiv \frac{|\sum_{i=1,n_R} \nu_{i,A}\omega_i \delta_B^i|}{\max(P_A, C_A)}, \tag{4}$$

where

$$P_A = \sum_{i=1,n_R} \max(0, \nu_{i,A}\omega_i), \tag{5}$$

$$C_A = \sum_{i=1,n_R} \max(0, -\nu_{i,A}\omega_i). \tag{6}$$

This coefficient is well defined and bounded between 0 and 1, which can be easily demonstrated:

$$\begin{aligned}\left|\sum_{i=1,n_R} \nu_{i,A}\omega_i \delta_B^i\right| &= \left|\sum_{i=1,n_R} \max\left(0, \nu_{i,A}\omega_i \delta_B^i\right)\right. \\ &\quad \left. - \sum_{i=1,n_R} \max\left(0, -\nu_{i,A}\omega_i \delta_B^i\right)\right| \\ &= |P_{AB} - C_{AB}|. \end{aligned} \tag{7}$$

The terms on the right-hand side correspond to the production and consumption of species A from reactions including species B. Then, as $0 \leqslant P_{AB} \leqslant P_A$ and $0 \leqslant C_{AB} \leqslant C_A$, it follows that $-C_A \leqslant P_{AB} - C_{AB} \leqslant P_A$, which is equivalent to $|P_{AB} - C_{AB}| \leqslant \max(P_A, C_A)$. This inequality simply means that the net contribution of a species B to a target species A cannot exceed the total production or consumption, whichever is larger, of species A.

As an example, let us consider the following extreme case. Suppose that species B is present in all consumption reactions for target A, but in none of its production reactions. If B is removed, A is produced, but not consumed anymore. The evolution of A will be significantly impacted only if the total consumption of A is at least comparable to its production. If $C_A \geqslant P_A$, $r_{AB} = 1$. If $C_A < P_A$, r_{AB} reduces to C_A/P_A, which directly compares production and consumption of A. If consumption is negligible compared with production, then B can be safely neglected. Fig. 1 compares the coefficients computed with Eq. (1), r^{DRG}, and with Eq. (4), r.

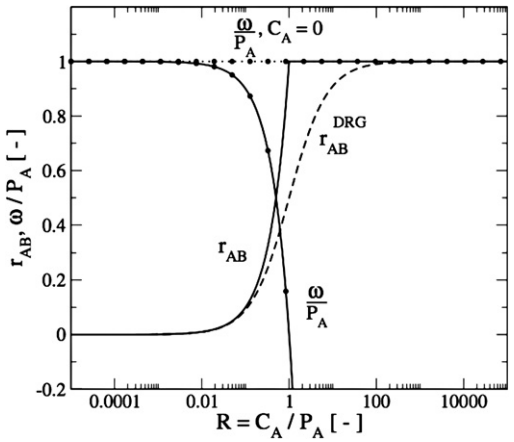

Fig. 1. Comparison of the direct interaction coefficients computed using Eq. (4) (r_{AB}, solid line) and using Eq. (1), (r_{AB}^{DRG}, dashed line) in the case of a species A being consumed exclusively through reactions containing species B. B is not involved in any production reaction for A. Also shown is the normalized source term of the evolution equation for species A, including (dotted, solid line) and neglecting (dotted, dashed line) species B.

For this case, both coefficients are similar when the production of A is dominant compared to its consumption. However, they start to differ when C_A is comparable to P_A, as r_{AB} increases faster than r_{AB}^{DRG} to reach 1 instead of 1/2 when $P_A = C_A$. Also shown in Fig. 1 is the comparison between the initial source term normalized by the production rate of A and the modified source term if B is removed. When $P_A = C_A$, the source term exhibits an error of 100% if B is removed, as indicated by $r_{AB} = 1$. In this case, the conventional DRG coefficient underestimates the contribution of B. r_{AB} quantifies how much removing B disturbs the established balance between production and consumption in the source term of A.

An interesting feature of this definition is that for a given species A, r_{AA} is not automatically unity. Keeping in mind that the coefficients are computed based on instantaneous reaction rate data, if A is in quasi-steady state, then the net production, i.e., the source term of the equation for the evolution of A is small. Setting it to 0 at that time would not introduce a significant error into the evolution of A. The coefficient r_{AA} is indeed small and goes to 0 as A approaches a quasi-steady state. On the other hand, if the consumption rate of A is small compared to its production rate, r_{AA} will approach unity.

2.2. Group-based direct interaction coefficients

Equation (4) provides an estimate of the impact that removing one species has on the calculated concentration of the remaining species. However, the goal

of the reduction procedure is to remove the largest possible set of species from the mechanism while keeping errors below a given tolerance. Considering one species independent of the group of removed species in which it will eventually belong might lead to a very inaccurate estimate of the importance of each species. The following example illustrates such a case.

A reactant A is consumed through four parallel reactions to form the four products $S_{i=1\ldots4}$. All the reactions have the same rate coefficient k:

$$(R_{i=1\ldots4}) \quad A \xrightarrow{k} S_i.$$

If species S_1, for instance, is removed from this mechanism, that is, reaction R_1 is removed, the relative error introduced in the consumption rate of A will be

$$\epsilon_{C_A} = \frac{4k[A] - 3k[A]}{4k[A]} = \frac{1}{4}. \tag{8}$$

This is in perfect agreement with the direct interaction coefficient between A and species S_1 given by Eq. (4):

$$r_{AS_1} = \frac{\omega_1}{\sum_{j=1}^{4} \omega_j} = \frac{1}{4}. \tag{9}$$

Suppose that an additional species S_2 is removed. The error in the rate of consumption of A is now $\epsilon_{C_A} = 1/2$. This is not well represented by the direct interaction coefficient $r_{AS_2} = 1/4$, because the definition from Eq. (4) does not take into account the contribution from the species S_1, previously removed. This observation leads to the extension of Eq. (4) given a set of removed species,

$$r_{AB,\{\mathcal{S}\}} \equiv \frac{|\sum_{i=1,n_R} \nu_{i,A}\omega_i \delta^i_{B,\{\mathcal{S}\}}|}{\max(P_A, C_A)}, \tag{10}$$

where $\{\mathcal{S}\}$ is the set of species already removed. $\delta^i_{B,\{\mathcal{S}\}}$ is unity if the ith reaction involves B or any species in subset $\{\mathcal{S}\}$, and 0 otherwise. Using this extended definition, the contribution for S_2 is now

$$r_{S_2} = \frac{\omega_1 + \omega_2}{\sum_{j=1}^{4} \omega_j} = \frac{1}{2}, \tag{11}$$

which is a better estimate of the effect of removing the group of species $\{S_1 + S_2\}$ from the mechanism.

2.3. Error propagation

For each species A present in a kinetic mechanism, a set of primary dependent species can be defined, consisting of the species that appear explicitly in elementary reactions involving A. The strength of the interaction between A and each species of this primary dependent set is defined by the interaction coefficient r_{AB} defined in Eq. (4). If a species B is not in the primary dependent set of A, then $r_{AB} = 0$.

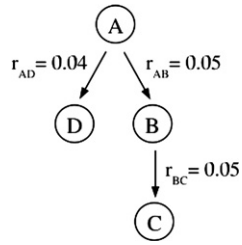

Fig. 2. Part of a directed relation graph involving four species. Although the link between species B and C is not the weakest in the graph, removing C should introduce the smallest error in the prediction of the target A.

Before discussing the error propagation method that has been developed in this work, it is interesting to look in more detail at the selection procedure used in the DRG methodology proposed by Lu and Law [10,21]. In the DRG method, a directed relation graph between species can be constructed, the strength of each edge from one species A to another species B being equal to the coefficient r_{AB}. Given a parameter ϵ representing the desired degree of reduction of the skeletal mechanism, any species reachable from a given set of targets through edges with strength greater than ϵ is included in the skeletal set of species. A more convenient way to formulate this DRG selection procedure is to assign directly to each species the value of ϵ above which the species is excluded automatically from the skeletal set. This value will be called R^{DRG}_{AB}. To do that, a path-dependent coefficient on a certain path p that links two species A and B, which are not necessarily directly related, can be defined as

$$r^{\mathrm{DRG}}_{AB,p} = \min_{i=1}^{n-1} r_{S_i S_{i+1}}, \tag{12}$$

with $S_1 = A$, $S_n = B$. For each path that leads from A to B, the weakest link is identified, so that above this threshold, the connection is severed and species B cannot be selected through this path. The definition of R^{DRG}_{AB} follows quite straightforwardly:

$$R^{\mathrm{DRG}}_{AB} \equiv \max_{\text{all paths } p} r^{\mathrm{DRG}}_{AB,p}. \tag{13}$$

Equations (12) and (13) highlight the fact that in the DRG species selection process, a path between A and B is fully characterized by its weakest contribution, regardless of its length. Intuitively however, the farther away from the target a species is, the smaller the effect of changing or removing this species should be. A simple example is depicted in Fig. 2.

Suppose species A is the target, and B and D are directly linked to A with coefficients 5% and 4%,

respectively. Another species C is directly linked to B with coefficient 5%. The weakest link being r_{AD}, species D would be the first species removed from the skeletal set in the DRG methodology, which introduces an estimated 4% error in the production rate of the target A. Still, removing species C would cause approximately a 5% error in species B that has to propagate through the graph to reach A. Doing so, this error is damped due to the weak contribution of B to the source term of target A. First removing C instead of D presumably introduces a smaller error in A, as C is not directly linked to the target. To take into account this error propagation process, a geometric damping has been introduced in the selection procedure. Equation (12) becomes

$$r_{AB,p} = \prod_{i=1}^{n-1} r_{S_i S_{i+1}}, \tag{14}$$

while Eq. (13) is left unchanged:

$$R_{AB} \equiv \max_{\text{all paths } p} r_{AB,p}. \tag{15}$$

If some error is introduced in the prediction of a species B, the longer the way this error has to propagate to reach the target A, the smaller its effect will be, typically. This technique is target-oriented and is expected to provide a finer selection of the chemical paths necessary for the accurate prediction of the set of targets by keeping species associated with large R coefficients and discarding species with small R coefficients. The validity of this error propagation assumption will be demonstrated in a subsequent section.

3. Reduction algorithm

As mentioned above, a skeletal mechanism is generated for a given set of targets over a given domain of applicability. Once those inputs are well-defined, the mechanism goes through several distinct reduction phases. The first phase is the selection of a subset of important species using the importance coefficient R presented above. This step is the most important one, as it reduces the number of differential equations that have to be solved. The second phase accelerates the computation of the remaining source terms by removing from the skeletal mechanism the reactions that have an overall negligible effect. An extra stage has been added here to reduce further the number of differential equations by replacing some of them by algebraic relations through quasi-steady state assumptions (QSSA). Suitable candidates for QSSA are identified using a lifetime analysis. It should be noted that this last stage of reduction is largely facilitated by the previous stage of removing individual reactions. QSSA leads to analytic expressions for all steady-state species. These expressions are often coupled and sometimes nonlinear. This implies the use of a solver for nonlinear systems, which can compromise the expected increase in computational efficiency.

3.1. Selection of species

3.1.1. Sampling process

The sampling of states in the parameter space, for which to perform the reduction process and for which to test the validity of the reduction, has to be chosen so that the union of samples adequately represents the parameter range of expected validity. The validity range of the reduced mechanism is either equal to or a subset of that of the detailed mechanism, but it cannot be larger. It is not clear exactly how to define the range of validity of a mechanism, but one possible standpoint could be to define it just as the set of conditions for which the mechanism has been validated with experimental data. Then also, the reduced mechanism is valid only at the same distinct locations in parameter space, which can easily be sampled. However, the sample size used here for the reduction process should be expanded. We will assume that the detailed chemical mechanism is valid in the vicinity of the data points included in the validation data set, such that it defines a domain. In a similar way, the reduced mechanism will be assumed also to be valid in that domain. A sample of states is chosen in the parameter space such that it can be reasonably assumed that the accuracy of the reduced mechanism between the sample points is represented by the accuracy of the scheme at the sample points. Strictly, this validity should be ensured by the method. Oluwole et al. [27,28], for instance, have developed a reduction technique based on constrained optimization that guarantees the range of validity of the reduced scheme. However, this approach is not applicable directly to the DRGEP method. Techniques that guarantee the validity of the reduced mechanism should be developed in the future.

As a further condition, all sample points should be easily computable. This implies that these are restricted to unsteady homogeneous reactor type configurations, such as those representing shock tube and flow reactor experiments, or one-dimensional configurations, such as laminar premixed or counterflow nonpremixed flames. This condition could be relaxed, but it would render the reduction procedure more costly. The computed states at the sample points are then characterized by the chosen set of values for the pertinent parameters and additionally are functions of time or space. The equations given below are written with time as the independent variable, but the time can

simply be replaced by a spatial coordinate for one-dimensional steady configurations.

The numerical solutions for all sample points are computed and the solutions are stored for further analysis. For this, it is important that a sufficient numerical accuracy is ensured, especially for premixed flames and unsteady ignition configurations. The DRGEP analysis can then be performed using the chemical production rate for each discrete point in time or space for a given sample point. However, since numerical accuracy is typically defined for a solution, even if a solution is smooth, the production rates for this solution might still exhibit numerical noise, such as oscillations, especially if nondissipative numerical schemes are used. Because of this, and to improve the computational time for the reduction algorithm, the production rate used in the reduction procedure are smoothed using a filter kernel that is substantially larger than the grid or time spacing, but much smaller than the total integration time or space. Here we typically use approximately 20 grid points or time intervals of the solution and perform a top-hat filtering. More elaborate filter kernels could be employed, but it is important to keep in mind that the filter width is defined not by a given length in time or space, but by the number of intervals, since most numerical chemistry solvers use adaptive methods in space and time. In the examples considered below, the filtering has consistently provided results similar to those of computing the coefficients at each point, but it decreases the computational time significantly.

3.1.2. Scaling

The DRGEP coefficients R_{AB} are relative quantities by construction. As a result, they do not differentiate between a solution point where the target has been consumed entirely and a solution point where target production or consumption is at its maximum. In the former case, the coefficients are meaningless; in the latter case, they can be crucial to get an accurate skeletal mechanism. To prevent ill-defined coefficients from overriding meaningful ones, a scaling factor α_T is defined that quantifies the contribution at a time t of each target T to the overall activity of the system. For this, we write the element balance resulting from chemical reactions as the difference of the contributions from reactions that consume species containing a certain element and reactions that produce species with this element. These pseudo-production and consumption rates can be written as

$$P_a = \sum_{\text{all species } S} N_{a,S} \max(0, P_S - C_S) \tag{16}$$

and

$$C_a = \sum_{\text{all species } S} N_{a,S} \max(0, C_S - P_S). \tag{17}$$

In these equations, a refers to different elements present in the system (C, H, O, and N for conventional hydrocarbon combustion), $N_{a,S}$ is the number of atoms a in species S, and P_S, and C_S are the production and consumption rates respectively of any species S. At each time, $P_a - C_a = 0$. The scaling coefficient associated with a specific atom a and target T is defined as

$$\alpha_{a,T}(t) = \frac{N_{a,T}|P_T - C_T|}{P_a}, \tag{18}$$

and the global normalized scaling coefficient is

$$\alpha_T(t) = \max_{\text{all atoms } a} \frac{\alpha_{a,T}(t)}{\max_t \alpha_{a,T}(t)}. \tag{19}$$

This scaling coefficient is unity when the target contributes to its maximum to the exchange of atoms between species, and zero when, for instance, the species mass fraction is constant, at chemical equilibrium, or when the target has been consumed entirely. To give an example, let us consider the rich homogeneous ignition of CO in air: as sole provider of carbon atoms, the fuel will have a scaling coefficient equal to unity, as long as it is consumed actively. When oxygen has disappeared, the fuel reaches a plateau, and its scaling coefficient rapidly decreases to zero. Such a scaling naturally overcomes problems of loss of significant digits, which happens at chemical equilibrium, as pointed by Lu and Law [25], and smoothes out the artificially large coefficients often encountered at early times, when some species are marginally produced through negligible paths.

Finally, the importance of a species S given a set of targets $\{\mathcal{T}\}$ and a set of sample points $\{\mathcal{D}\}$ is quantified by a single parameter defined as

$$\overline{R_S} = \max_{\substack{T\in\{\mathcal{T}\}\\ k\in\{\mathcal{D}\}}} (\alpha_{T,k} R_{TS,k}). \tag{20}$$

The maximum norm has been selected for its universality over different physical conditions and targets. Species associated with the smallest coefficients $\overline{R_S}$ are removed first and these coefficients are periodically reevaluated during the reduction procedure to take advantage of the group-based direct interaction coefficients.

3.1.3. Integrity check

Every intermediate species in a skeletal mechanism must have at least one production and one consumption path. During the DRGEP reduction process, some species might fail this requirement, especially for high reduction ratios in the context of complex, highly nonlinear kinetic schemes. Two basic observations can be made. In a closed system, any intermediate species that is not produced any more remains at

its initial zero concentration and can be removed from the mechanism. On the other hand, if a species is produced, but not consumed anymore, it creates a sink of mass that may impact greatly the final concentration of the products. This complex nonlinear behavior cannot be detected by a method based solely on the analysis of the detailed production rates. That is why a simple algorithm has been designed to prevent these situations from occurring. A list of species, sorted by order of importance for the targets, is first obtained by computing the DRGEP coefficients using Eq. (4). Then this list is slightly modified so that, for any value of the cutoff parameter, the group of species kept in the skeletal mechanism forms a consistent chemical scheme with no truncated paths. The reordering proceeds as follows.

Species are moved to the set of removed species one after the other, starting from the less important ones. For each candidate species A to be removed, the integrated production and consumption rates of the species S_i directly linked to A are reevaluated using the detailed data by setting the contribution from species A to zero. If the integrated production rate of S_i is less than a percent of its detailed value, that is, S_i is virtually not produced anymore, S_i is linked to species A, and the two-species group is assigned the DRGEP coefficient of species A. If any one of the species in the group is removed, the rest of the group is removed as well. A similar grouping procedure is adopted when S_i is not consumed anymore, except that the $\{S_i, A\}$ group is assigned the larger DRGEP coefficient R_{S_i}; that is, the group is moved up in the ordered list.

During the reordering sweep, DRGEP coefficients are recomputed regularly using the group-based definition given in Eq. (10). All the computations during this stage are based solely on the detailed data; no reduced solution is computed. The list of individual and indivisible groups of species obtained at the end of the integrity check is used to evaluate skeletal mechanisms of various sizes to get the shortest mechanism satisfying the accuracy requirements.

3.1.4. Theoretical examples

The applicability of the directed relation graph method has been extensively reviewed by Lu and Law [25]. A number of generic cases including quasi-steady-state, partial equilibrium, and dormant mode problems were analyzed in detail using DRG. The present error propagation method leads to similar, equally good conclusions for these cases, which can be demonstrated very easily. This will be shown here in two examples. The first one considers an artificial reaction mechanism in which an intermediate species is in quasi-steady state:

$$\begin{aligned}
&(R_1) \qquad F \to R, \quad \omega_1 = 1 \cdot [F],\\
&(R_2) \qquad R \to P, \quad \omega_2 = 10^3 \cdot [R],\\
&(R_3) \qquad R \to P', \quad \omega_3 = 1 \cdot [R].
\end{aligned} \tag{21}$$

The rates of the reactions were evaluated in [25] as $\omega_2 \approx \omega_1$ and $\omega_3 = \omega_2/10^3$. The direct interaction coefficients defined by Eq. (4) are

$$\begin{aligned}
r_{FR} &= \frac{\omega_1}{\max(P_F, C_F)} = \frac{\omega_1}{\omega_1} = 1,\\
r_{RF} &= \frac{\omega_1}{\max(P_R, C_R)} = \frac{\omega_1}{\omega_1} = 1;\\
r_{RP} &= \frac{\omega_2}{\max(P_R, C_R)} = \frac{\omega_2}{\omega_1} = 1,\\
r_{PR} &= \frac{\omega_2}{\max(P_P, C_P)} = \frac{\omega_2}{\omega_2} = 1;\\
r_{RP'} &= \frac{\omega_3}{\max(P_R, C_R)} = \frac{\omega_3}{\omega_1} \approx 10^{-3},\\
r_{P'R} &= \frac{\omega_3}{\max(P_{P'}, C_{P'})} = \frac{\omega_3}{\omega_3} = 1.
\end{aligned} \tag{22}$$

If species F is the target, the corresponding DRGEP coefficients are obtained straightforwardly:

$$\begin{aligned}
R_{FR} &= r_{FR} = 1,\\
R_{FP} &= r_{FR} \cdot r_{RP} = 1,\\
R_{FP'} &= r_{FR} \cdot r_{RP'} \approx 10^{-3}.
\end{aligned} \tag{23}$$

The right conclusion can be derived from these coefficients; that is, species P' can be safely removed; it will not introduce a large error in the prediction of F. But both R and P should be kept in the mechanism.

Another case of interest is the rapid conversion of a reactant into a product through a succession of quasi-steady-state intermediates. This case was handled correctly by the DRG method, but not by the error propagation method presented in [26]. Let us consider a path from a fuel F to a product P that goes through several intermediate species R_1 to R_n, as depicted in the following mechanism:

$$\begin{aligned}
F \xrightarrow[\omega_0]{k_0=1} R_1 \xrightarrow[\omega_1]{k_1=1/\epsilon} R_2 \xrightarrow[\omega_2]{k_2=1/\epsilon} \cdots\\
\xrightarrow[\omega_{n-1}]{k_{n-1}=1/\epsilon} R_n \xrightarrow[\omega_n]{k_n=1/\epsilon} P.
\end{aligned} \tag{24}$$

The rate-limiting step is the first reaction, and the remaining reactions are fast, so that all species $R_{i,i=1,n}$ can be considered as in quasi-steady state. Thus, the rates of all reactions appearing in the mechanism (24) are approximately equal:

$$\omega_0 \approx \omega_1 \approx \cdots \approx \omega_n \approx \omega. \tag{25}$$

As a species R_i is produced only by R_{i-1}, and is consumed to produce one single species R_{i+1},

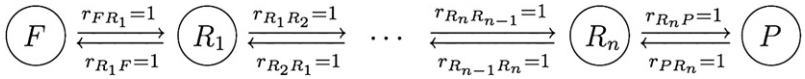

Fig. 3. Direct interaction coefficients between species involved in mechanism (24).

$\max(\omega_i, \omega_{i-1}) = \omega$, and all direct interaction coefficients $r_{R_i R_{i\pm1}}$ are unity. Fig. 3 shows the corresponding relation graph.

From this figure, the effect of the fuel F on the product P described by the DRGEP coefficient R_{PF} is

$$R_{PF} = r_{PR_n} \cdot r_{R_nR_{n-1}} \cdot \cdots \cdot r_{R_2R_1} \cdot r_{R_1F} \approx 1. \quad (26)$$

The importance of F to P, as the only source of production for P, is recovered thanks to the more appropriate definition of the direct interaction coefficients. Thus, in this example, if P is the target, no species can be removed, as removing the fuel or any intermediate species would introduce a 100% error into the prediction of the product P.

3.2. Selection of reactions

Removing species decreases the number of differential equations that have to be solved, and, since the computational time scales as the square of the number of species, this is the most efficient way to speed up numerical simulations. However, the computational time also depends on the number of reactions, which can be significant. In addition, as mentioned before, the elimination of elementary reactions renders the introduction of steady state species more efficient. The first step of reduction provides the set of species that have to be kept in the system to achieve the desired accuracy. Thus, the resulting mechanism is made up of all reactions among those species. However, not all reactions are necessary for an accurate representation of the original dynamic system. Specifically, the importance of a reaction depends on the contribution to the involved species and the importance of those species for the targets. This information is used to identify reactions that have minimal impact on the targets, and thus can be removed safely. For this stage, backward and forward reactions are considered as being independent from one another.

A strategy similar to the one used for species selection is adopted here. The direct interaction coefficient between a species A and a reaction r_i is written as

$$r_{Ar_i} \equiv \frac{|\nu_{i,A}\omega_i|}{\max(P_A, C_A)}. \quad (27)$$

Then the impact of removing reaction r_i on a given target T is evaluated through error propagation using the DRGEP coefficients for the species, as

$$R_{Tr_i} \equiv \max_{S\in\{\mathcal{S}\}} (R_{TS} r_{Sr_i}), \quad (28)$$

where $\{\mathcal{S}\}$ refers here to the set of species present in the mechanism. The reactions are sorted by increasing order of importance using the single parameter

$$\overline{R}_{r_i} = \max_{\substack{T\in\{\mathcal{T}\}\\ k\in\{\mathcal{D}\}}} (\alpha_{T,k} R_{Tr_i,k}). \quad (29)$$

Equations (27) and (28) are extended easily to take into account the set of already discarded reactions, as is done for species in Eq. (10). The coefficients $\overline{R}_{r_i}$ are recomputed regularly to take advantage of these group-based coefficients. An integrity check is performed during the reaction reduction to ensure that every species remaining in the mechanism retains at least one major production and one major consumption path for the physical conditions considered in the reduction. The species are represented more or less accurately depending on their own global importance for the targets. An additional limited number of species might be removed during the reaction reduction when high reduction ratios are reached.

3.3. QSS species selection

To additionally increase the speed-up of the resulting skeletal mechanism, a straightforward strategy is the introduction of quasi-steady-state assumptions that replace part of the differential equations with algebraic equations, which are much faster to evaluate. Several methods for systematically identifying suitable QSS species can be found in the literature [29,30]. In the present work, a steady state parameter based on lifetime analysis has been chosen, which is very similar to the level of importance (LOI) criterion presented in [30,31]. Because of the number of cases and the typical size of the skeletal mechanisms obtained after the DRGEP reduction, sensitivity coefficients are still very expensive to compute. On the other hand, scaled, time-dependent DRGEP coefficients are readily available and are used in place of sensitivity coefficients. The steady state parameter Q can be expressed as

$$Q_S(t) = \alpha_T R_{TS}[S]\theta_S, \quad (30)$$

where

$$\theta_S = -\left[\frac{\partial(P_S - C_S)}{\partial[S]}\right]^{-1} \quad (31)$$

is a measure of the life time of species S and $[S]$ is its concentration. As suggested in [30,31], the species with small Q values for all cases can be set in steady state. For simplicity, only linear coupling between steady state species is allowed, so that explicit expressions can be written automatically for direct use in a combustion code. Still, the application of steady state assumptions for nonlinearly coupled species can often lead to very good results, especially since recent work has focused on the optimization of the extra cost associated with the evaluation of the nonlinear quasi-steady state equations [32].

3.4. Error measure

As Valorani et al. [24] noticed, a meaningful error measure is a crucial, yet often ill-defined quantity for temporally or spatially unbounded problems. For instance, in the case of homogeneous ignition, the relative error in ignition delay time is not a monotonic function of the size of the skeletal mechanism, and a small error in ignition timing does not mean that the skeletal mechanism reproduces the dynamics of the detailed mechanism accurately. Moreover, evaluating the error made on intermediate species is nontrivial. The most commonly used approach is to shift the skeletal solution so that some important parameter matches before computing a normalized integral of the difference between both solutions. For temporally or spatially unbounded cases, however, this integral depends on the length of the domain, which can vary when the mechanism is reduced.

To remedy those problems, a more efficient approach has been proposed in [24], which consists in computing this error in phase space. This implies finding a well-behaved mapping variable that uniquely parameterizes both detailed and skeletal solutions. To get meaningful measures, this variable needs to be independent from the quantities whose error is needed, vary smoothly between two fixed values, and be nonconstant over the domain of interest. In [24], the fuel is used as independent coordinate. This transformation is adequate as long as the fuel is actively consumed, but is singular elsewhere. As a result, in ignition simulations, for example, intermediate species, or even products whose production occurs later in the ignition process, are not well represented in phase space, and a major contribution of the error is missing. Moreover, this mapping cannot be used to evaluate the error made in fuel concentration itself.

In this work, a systematic way of measuring errors for temporally or spatially unbounded cases, such as homogeneous reactors or freely propagating flames, has been designed that adapts the error measure to the characteristics of the variables for which an error has to be computed. Global parameters such as burning velocities or ignition delay times are compared using relative differences:

$$E_G = \left| \frac{G_{\text{det}} - G_{\text{red}}}{G_{\text{det}}} \right|. \tag{32}$$

Species are divided into two distinct subsets. The first subset includes any species whose contribution to the mixture at chemical equilibrium is negligible, namely all reactants and intermediates. For this type of variable, the integrated error with respect to a common progress variable Y_C is applicable. The progress variable is formed based on the major products obtained in the simulation. When this progress variable is well chosen, it stretches the ignition zone, where most of the changes occur, and is well-defined during the early stages, thanks to the early release of some of the combustion products, such as H_2O. The species used to define the progress variable and the minor products form the second subset.

A major issue of error estimation based on a change of coordinate is that the error of species used for the progress variable, or even products that behave like the progress variable, cannot be estimated in the same way as the intermediates, as the mapping coordinate cannot be assumed to be independent anymore. A first meaningful quantity to compare is the value of the variable at chemical equilibrium. To appraise the differences in the formation of the products, the integrated error between detailed and reduced solution in terms of the spatial or temporal coordinate is used. In an effort to remove any ambiguity, however, the reduced solution is rescaled twice: in amplitude, to recover the same chemical equilibrium, and in time, to get the same characteristic time scale τ, ignition time or 95% of total fuel consumption, for instance. Combined with the relative error in the chemical equilibrium, this error measure provides direct information on the number of changes introduced in the skeletal model. In this work, any relative error larger than 100%, indicating very bad agreement between detailed and reduced solutions, is clipped to 100%. For ignition delay time, for example, 100% error means either that the relative difference between the detailed and reduced solution is larger than 100%, or that no ignition occurs when using the reduced scheme.

4. Practical examples

4.1. Validation of the error propagation assumption

Before applying the above reduction methodology, it is necessary to appraise the validity of the error propagation assumption in the DRGEP method. This assumption states that the effect on a target introduced

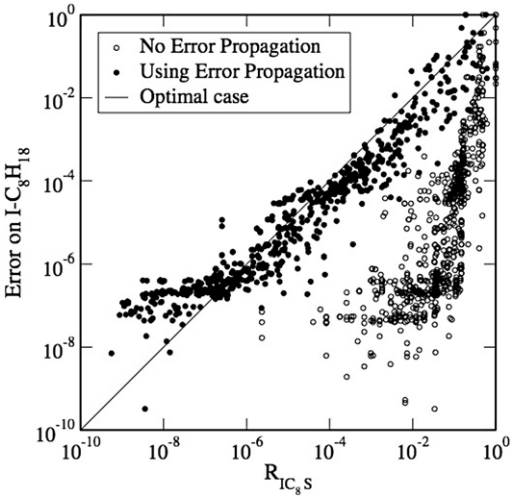

Fig. 4. Correlation between the error introduced in the fuel prediction and the species coefficients R_{IC_8S} obtained with or without error propagation during the isochoric, adiabatic autoignition of a stoichiometric mixture of iso-octane and air at 13 bar and 1000 K.

by the removal of a species can be approximated through geometric damping along the directed relation graph, from the target to the removed species. This can be written as

$$E_T \propto R_{TS}, \tag{33}$$

where E_T is the error between the prediction of the target using the detailed and skeletal mechanisms, and R_{TS} measures the importance of a species S with respect to the target, as defined by Eqs. (4) and (15). This proportionality can be verified *a posteriori* using a practical case. The case was chosen randomly among the numerous conditions used for the reduction of the LLNL iso-octane mechanism. The coefficients R_{TS} were computed for the adiabatic, isochoric autoignition of a stoichiometric mixture of iso-octane and air at 13 bar and 1000 K, with iso-octane as the only target. Then, the error introduced in the prediction of iso-octane by removing each species individually was computed using the integrated error measure introduced in Section 3.4. The progress variable Y_C for this case is the sum of CO, CO_2, and H_2O mass fractions.

Fig. 4 shows the correlation between this error and the computed coefficients obtained using error propagation. For comparison, the correlation between the error and the coefficients obtained without error propagation is also shown in the same figure. These coefficients are obtained using the definition for r_{AB} from Eq. (4) and the DRG selection method used by Lu and Law (Eq. (13)). The solid line represents the optimal case, that is, a hypothetical parameter whose value would be exactly equal to the error introduced if the species were removed.

Several comments can be made at this point. First, a very small error, on the order of 10^{-7}, is introduced systematically due to numerics and grid resolution. This accounts for the asymptote observed in Fig. 4 for relatively small R coefficients. The coefficients obtained using error propagation are smaller than those obtained without propagation, as geometric damping is used to evaluate them. The errors introduced by removing individual species correlate extremely well with the error propagation coefficients, with a small scatter in the data, whereas the correlation is not as obvious when the DRG selection procedure is used. Fig. 4 also shows that the error propagation method leads to an order unity coefficient in Eq. (33), while the original DRG method does not. This means that the importance coefficients evaluated by DRGEP are a direct measure for the error in the resulting mechanism. However, a more detailed analysis is needed here to appraise the performances of both methods.

For a given value $R^{\text{ref}}_{IC_8S}$ of the selection parameter, the species can be divided into three groups. The first group contains the species whose coefficients are smaller than $R^{\text{ref}}_{IC_8S}$. These species are labeled "identified minor" species. $\text{Err}^{\max}_{\text{I-C}_8\text{H}_{18}}$ is defined as the maximum error introduced by one of the identified minor species. It is important to note that $\text{Err}^{\max}_{\text{I-C}_8\text{H}_{18}}$ is different from the error obtained when removing the whole minor species group, as the system is highly non-linear. This issue is dealt with using the group-based coefficient technique that will be validated in the next section. The remaining species, for which $R > R^{\text{ref}}_{IC_8S}$, are divided into two further groups: the species that introduce an error larger than $\text{Err}^{\max}_{\text{I-C}_8\text{H}_{18}}$, and those introducing a smaller error. The latter species are labeled "nonidentified minor" species, as they could have been included in the minor species set without increasing the maximum individual error $\text{Err}^{\max}_{\text{I-C}_8\text{H}_{18}}$. These subdivisions are detailed in Fig. 5a, that is a close-up view of Fig. 4.

A good selection parameter limits the number of nonidentified minor species as much as possible, to ensure that for a given value of the cutoff parameter, the maximum number of species is selected, introducing the smallest possible error. This efficiency can be quantified by the ratio between the number of identified minor species and the number of species that should have been identified as minor, that is, the total number of identified and nonidentified minor species. Using Fig. 5a as an example, this means comparing the number of species contained in the lower left quadrant to the number of species in the lower half

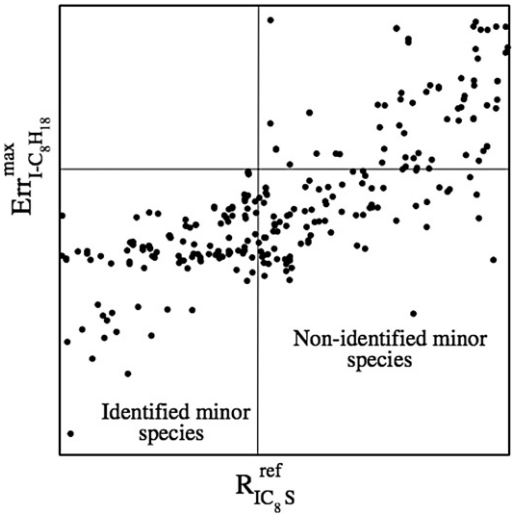

(a)

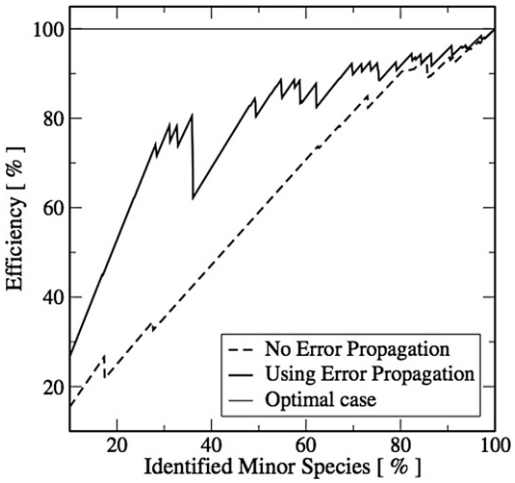

(b)

Fig. 5. Validation of the error propagation assumption. (a) Close-up view of Fig. 4. (b) Selection of minor species. Comparison between DRG selection and error propagation selection.

of the graph, for an increasing value of the cutoff parameter R_{IC_8S}, that is, for an increasing number of species identified as minor.

The results are shown in Fig. 5b. The optimal case corresponds to a constant value of 100%, as all the species that can be classified as minor are identified. Also, an error-propagation-based selection parameter clearly is more efficient than the standard DRG selection. This result can be interpreted in two ways. The first one is that for a given number of species selected as minor, the maximum individual error over those species is larger when DRG is used than when the error propagation method is used. Or conversely, for a given maximum error, more species introducing an error smaller than this maximum are identified using error propagation than using DRG.

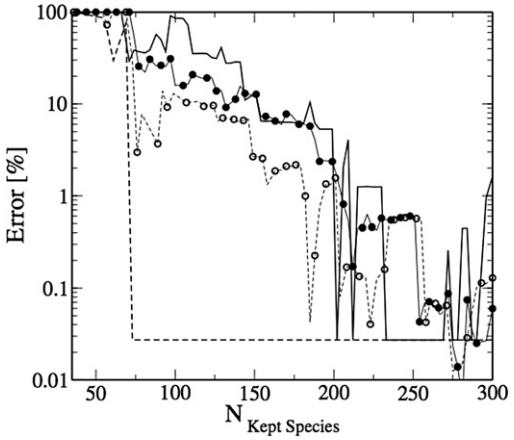

Fig. 6. Iso-octane autoignition at low temperature. Evolution of the error in ignition delay time (lines with symbols) and final mass fraction of CO (plain lines) when the group-based coefficients and the integrity check algorithm are used (open symbols, dashed lines) or not (filled symbols, solid lines).

This analysis shows that the error propagation assumption can be considered as valid and appropriate, and represents a significant improvement over the species selection presented in earlier work [21,25].

4.2. *Efficiency of group-based coefficients and integrity check*

The efficiency of the group-based coefficients and the integrity check is illustrated next. The detailed mechanism for iso-octane oxidation from LLNL [33] is reduced for a single initial physical condition, the homogeneous, adiabatic autoignition at constant volume of a stoichiometric mixture of iso-octane and air at an initial pressure of 13 bar and an initial temperature of 625 K. The targets are fuel, CO, CO_2, and temperature. Fig. 6 shows the evolution of the error in ignition delay time and in the final mass fraction of carbon monoxide as function of the number of species kept in the skeletal mechanism.

When the definition of Eq. (4) is used, the error in the final mass fraction of CO in the system quickly reaches a few percent and keeps increasing. This is due to truncated chemical paths appearing as species are removed. Carbon mass accumulates in large quantities in intermediate species, which shifts considerably the chemical equilibrium of the system. When group-based coefficients and integrity check are included in the reduction process (the coefficients are recomputed once every 50 species removed), the error in the final mass fraction of CO remains ex-

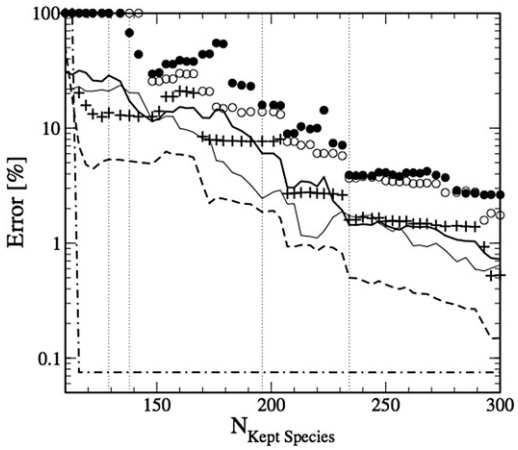

Fig. 7. Iso-octane autoignition. Evolution of the maximum (symbols) and average (lines) errors on ignition delay time (bold line, filled circles), first-stage ignition delay time (thin line, open circles), and fuel profile (dashed line, plus signs) as function of the number of species during the reduction of the iso-octane mechanism. The dash–dotted line represents the error of the final value of the progress variable Y_C. Dotted vertical bars indicate the sizes of the skeletal mechanisms used in the comparison shown in Fig. 8.

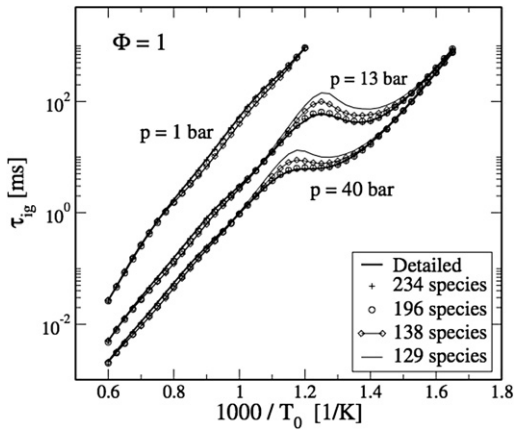

Fig. 8. Comparison of ignition times obtained with the detailed iso-octane mechanism and skeletal mechanisms of various sizes.

tremely small and the error in ignition delay time is improved considerably.

4.3. Iso-octane autoignition

To demonstrate the full capabilities of the DRGEP method, the same very large mechanism for iso-octane oxidation [33] is reduced for adiabatic autoignition at constant volume in a large range of initial conditions relevant for engine-related applications (ignition delay times less than 1 s). The initial conditions include equivalence ratios between 0.5 and 2, pressures between 1 and 40 bar, and temperatures between 600 and 1500 K. The detailed mechanism comprises 850 species and 7212 reactions. Targets for the reduction are fuel i-C_8H_{18}, major products CO and CO_2, and temperature. The DRGEP coefficients for temperature are evaluated using heat release data. The error in ignition delay time, first-stage ignition delay time, and the maximum error in the final value of the major products appearing in the definition of the progress variable Y_C are shown as functions of the number of species kept in the skeletal mechanism in Fig. 7. The progress variable is case-dependent and includes the major products of the simulation, so that it contains at least 90% of the carbon, oxygen, and hydrogen mass present in the system. Usually, CO_2 and H_2O are used, with CO and H_2 added when needed.

Overall, errors are increasing monotonically as the number of species is reduced. Error in the progress variables is everywhere small enough to neglect any effect on the change of coordinates for the detailed and skeletal mechanisms. Fig. 8 shows a comparison of the ignition delay time over a wide range of temperature and pressure for stoichiometric mixtures for several sizes of the skeletal mechanism, namely 234, 196, 138, and 129 species. For clarity, vertical bars have been added at the corresponding abscissas in Fig. 6. The 234- and 196-species mechanisms correspond to the smallest mechanisms with a maximum error of less than 5% and 15%, respectively; the 138-species mechanism is the smallest mechanism with an average error of less than 15%, and the 129-species mechanism is the smallest mechanism for which ignition occurs at all, even if not accurate, for all cases in the mechanism.

It can be seen that the high- and low-temperature regions are reproduced very well, even for very small mechanisms. However, the negative temperature coefficient region, which is the most sensitive to perturbations, concentrates the largest errors.

The total number of species kept for the first stage of reduction is chosen so that the maximum error over all targets is about 15%, which corresponds to 196 remaining species and 1762 remaining reactions, forward and backward counted separately. Following this first step of reduction and with the same accuracy requirement, additional non-necessary reactions are removed, and the resulting skeletal mechanism comprises 195 species and 802 reactions.

The final stage of reduction aims to identify species that can be set in steady state. The values for the steady state parameter Q are computed for all cases and targets using Eq. (30) and used to identify suitable candidates. To assess the potential of the method, the actual error on the final temperature is computed for a selected set of cases when setting species to steady state one after the other. This er-

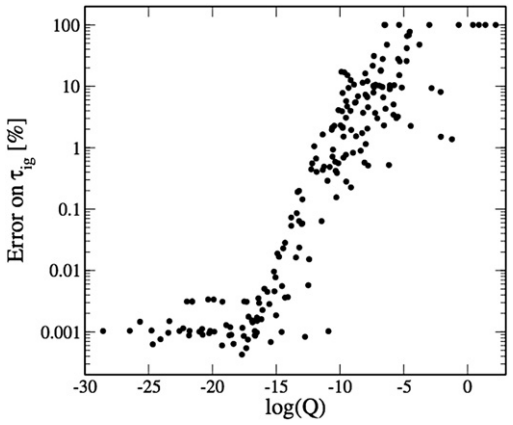

Fig. 9. Maximum error in ignition delay time against the steady state parameter Q of each species when set in steady state over the specified range of initial conditions used for the reduction of the iso-octane mechanism.

Table 1
Maximum and average errors for various skeletal and reduced mechanisms for initial conditions with pressures between 1 and 40 bar, equivalence ratios between 0.5 and 2, and temperatures between 600 and 1500 K

$N_{Species}$	$N_{Reactions}$	$N_{QSS\ species}$	Maximum error (%)	Average error (%)
196	1762	0	15.89	6.02
195	802	0	14.96	5.55
100	802	95	15.28	6.13

ror is correlated with the corresponding value of Q for the species. Results are presented in Fig. 9.

A very small error, of order 10^{-5}, is introduced systematically, that is, due to numerics and grid resolution. A clear trend is observed, with species having small Q values introducing comparatively smaller error than species with large Q values. For example, a cutoff value of $Q = 10^{-12.25}$ identifies correctly 80 out of 83, that is, 96% of the species introducing less than 0.2% error in ignition delay time when set in steady state. As mentioned above, species introducing quadratic coupling in the QSS equations are removed from the selected set. Among the 195 present species, a total of 95 species are identified as good candidates, so that no quadratic coupling is introduced in the algebraic system. The algebraic equations are decoupled and written explicitly by reordering the QSS species and solving the few small coupled sets using exact Gauss pivoting, following an approach similar to that presented by Lu and Law [34].

The maximum and average errors over the desired domain of applicability obtained using the skeletal mechanism at its various stages of reduction are summarized in Table 1.

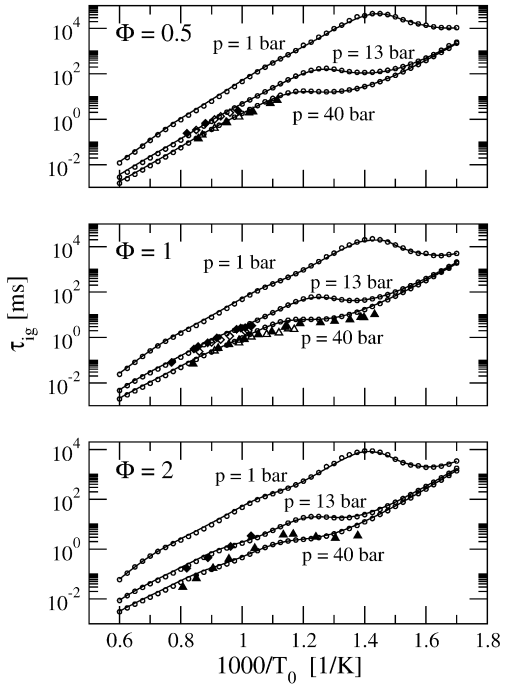

Fig. 10. Performance of the iso-octane mechanism obtained at the end of the reduction procedure: comparison between the detailed (solid line) and reduced (circles) mechanisms along with experimental data (filled symbols from Fieweger et al. [36], open symbols from Hanson and co-workers [35]).

The comparison between the ignition delay times obtained over the same parameter range using the detailed and the reduced mechanisms is shown in Fig. 10, along with experimental shock tube data [35,36].

The reduced mechanism reproduces correctly the detailed ignition behavior, with differences that are negligible compared to the discrepancies with experimental data, even for very long ignition delay times that were not included in the reduction procedure.

5. Conclusion

An error propagation method has been proposed and evaluated for the systematic and fully automatic reduction of large kinetic mechanisms. Coupled with a directed relation graph method, the technique allows a finer selection of the chemical paths important for a set of targets. Adequate scaling and consistency checks have been introduced that greatly enhance the efficiency of the reduction procedure. An additional module that identifies suitable quasi-steady-state species and that automatically produces efficient QSS equation evaluation code has been added. As an example, a 195-species skeletal and a 100-

species reduced mechanism for iso-octane autoignition have been extracted from a 850-species detailed mechanism while introducing overall small errors in fuel consumption, product concentrations, and ignition delay times.

Acknowledgment

Funding by the Air Force Office of Scientific Research is gratefully acknowledged.

References

[1] W.J. Pitz, N.P. Cernansky, F.L. Dryer, F.N. Egolfopoulos, J.T. Farrell, D.G. Friend, H. Pitsch, SAE 2007-01-0175 (2007).
[2] J.T. Farrell, N.P. Cernansky, F.L. Dryer, D.G. Friend, C.A. Hergart, C.K. Law, R.M. McDavid, C.J. Mueller, A. Patel, H. Pitsch, SAE 2007-01-0201 (2007).
[3] E. Eddings, S. Yan, W. Ciro, A. Sarofim, Combust. Sci. Technol. 177 (2005) 715–739.
[4] M. Colket, T. Edwards, S. Williams, N. Cernansky, D. Miller, F. Egolfopoulos, P. Lindstedt, K. Seshadri, F. Dryer, C. Law, D. Friend, D. Lenhert, H. Pitsch, A. Sarofim, M. Smooke, W. Tsang, AIAA 2007-770 (2007).
[5] H. Pitsch, N. Peters, SAE 98-2464 (1998).
[6] U. Müller, Ph.D. thesis, Rheinische-Westpölische Technische Hochschule Aachen, Germany (1993).
[7] M. Valorani, F. Creta, D. Goussis, J. Lee, H. Najm, Combust. Flame 146 (2006) 29–51.
[8] A.S. Tomlin, T. Turányi, M.J. Pilling, Mathematical Tools for Construction, Investigation and Reduction of Combustion Mechanisms, Elsevier, Amsterdam, 1998.
[9] M. Frenklach, Reduction of Chemical Reaction Models, American Institute of Aeronautics and Astronautics, Inc., Washington, DC, 1991, chap. 5, pp. 129–154.
[10] T. Lu, C. Law, Proc. Combust. Inst. 30 (2005) 1333–1341.
[11] J. Luche, M. Reuillon, J.-C. Boettner, M. Cathonnet, Combust. Sci. Technol. 176 (2004) 1935–1963.
[12] H. Soyhan, F. Mauss, C. Sorusbay, Combust. Sci. Technol. 174 (2002) 73–91.
[13] T. Turányi, New J. Chem. 14 (1990) 795–803.
[14] I.G. Zsély, T. Turányi, Phys. Chem. Chem. Phys. 5 (2003) 3622–3631.
[15] B. Bhattacharjee, D. Schwer, P. Barton, W. Green, Combust. Flame 135 (2003) 191–208.
[16] Y.F. Tham, J.Y. Chen, Fall Meeting of the Western States Section of the Combustion Institute (2003).
[17] H. Wang, M. Frenklach, Combust. Flame 87 (1991) 365–370.
[18] N. Peters, B. Roggs, Reduced Kinetic Mechanisms for Applications in Combustion Systems, Lecture Notes in Physics, Springer-Verlag, New York, 1992.
[19] U. Maas, S. Pope, Combust. Flame 88 (1992) 239–264.
[20] S. Lam, D. Goussis, Int. J. Chem. Kinet. 26 (1994) 461–486.
[21] T. Lu, C. Law, Combust. Flame 144 (2006) 24–36.
[22] M. Valorani, F. Creta, H. Najm, D. Goussis, Comput. Fluid Solid Mech. (2005) 900–904.
[23] M. Valorani, F. Creta, F. Donato, H. Najm, D. Goussis, Proc. Combust. Inst. 31 (2006) 483–490.
[24] M. Valorani, F. Creta, F. Donato, H. Najm, D. Goussis, European Conference on Computational Fluid Dynamics, ECCOMAS CFD (2006).
[25] T. Lu, C. Law, Combust. Flame 146 (2006) 472–483.
[26] P. Pepiot, H. Pitsch, 4th Joint Meeting of the U.S. Sections of the Combustion Institute (2005).
[27] O.O. Oluwole, B. Bhattacharjee, J.E. Tolsma, P.I. Bartona, W.H. Green, Combust. Flame 146 (2006) 348–365.
[28] O.O. Oluwole, P.I. Bartona, W.H. Green, Combust. Theory Modelling 11 (2007) 127–146.
[29] T. Turányi, A.S. Tomlin, M.J. Pilling, J. Phys. Chem. 97 (1993) 163–172.
[30] T. Lovas, D. Nilsson, F. Mauss, Proc. Combust. Inst. 28 (2000) 1809–1815.
[31] T. Lovas, P. Amneus, F. Mauss, E. Mastorakos, Proc. Combust. Inst. 29 (2002) 1387–1393.
[32] A. Arvidsson, T. Lovas, F. Mauss, Third European Combustion Meeting ECM (2007).
[33] H.J. Curran, P. Gaffuri, W.J. Pitz, C.K. Westbrook, Combust. Flame 129 (2002) 253–280.
[34] T. Lu, C. Law, J. Phys. Chem. A 110 (2006) 13202–13208.
[35] D. Davidson, B. Gauthier, R. Hanson, Proc. Combust. Inst. 30 (2005) 1175–1182.
[36] K. Fieweger, R. Blumenthal, G. Adomeit, Combust. Flame 109 (1997) 599–619.